REPORT DOCUMENTATION PAGE

Form Approved
OMB NO. 0704-0188

1. AGENCY USE ONLY (Leave Blank)	2. REPORT DATE	3. REPORT TYPE AND DATES COVERED
	24 July 2003	Peer Reviewed Reprint

4. TITLE AND SUBTITLE
Adaptive-Rate Turbo Product Coding for Frequency-Hop Transmission and Time-Varying Partial-Band Interference

5. FUNDING NUMBERS
DAAD19-99-1-0289

6. AUTHOR(S)
Michael B. Pursley

7. PERFORMING ORGANIZATION NAME(S) AND ADDRESS(ES)
Electrical and Computer Engineering
Clemson University
303 Fluor Daniel Building
Clemson, SC 29634

8. PERFORMING ORGANIZATION REPORT NUMBER

9. SPONSORING / MONITORING AGENCY NAME(S) AND ADDRESS(ES)
U. S. Army Research Office
ATTN: AMSRL-R0-S (TR)
P.O. Box 12211
Research Triangle Park, NC 27709-2211

10. SPONSORING / MONITORING AGENCY REPORT NUMBER
39007-CI
.16

11. SUPPLEMENTARY NOTES
The views, opinions and/or findings contained in this report are those of the author(s) and should not be construed as an official Department of the Army position, policy or decision, unless so designated by other documentation.

12 a. DISTRIBUTION / AVAILABILITY STATEMENT
Approved for public release; distribution unlimited.

12 b. DISTRIBUTION CODE

13. ABSTRACT (Maximum 200 words)
A protocol is described and evaluated for adapting the rate of a turbo code for frequency-hop packet transmissions over time-varying partial-band interference channels. The rate of the turbo code is adapted from packet to packet to optimize the throughput. In particular, the protocol is designed to use a high-rate code when there is little interference and a low-rate code when the interference occupies a significant fraction of the band, even though neither the transmitter nor the receiver know what fraction of the band contains interference. No external side information is provided to the receiver, and our scheme requires no additional redundancy (e.g., pilot symbols) in the data packet for the generation of side information. The information needed to adapt the code rate is derived from our adaptive decoding system, and the only feedback required from the receiver to the transmitter is provided by a few bits in each acknowledgment packet. Results on the performance of the protocol are given from turbo product codes.

14. SUBJECT TERMS
frequency-hop packet transmissions, adaptive decoding system, side information

15. NUMBER OF PAGES
6

16. PRICE CODE

17. SECURITY CLASSIFICATION OR REPORT	18. SECURITY CLASSIFICATION ON THIS PAGE	19. SECURITY CLASSIFICATION OF ABSTRACT	20. LIMITATION OF ABSTRACT
UNCLASSIFIED	UNCLASSIFIED	UNCLASSIFIED	UL

To appear in the *Proceedings of the 2003 IEEE Military Communications Conference*

Adaptive-Rate Turbo Product Coding for Frequency-Hop Transmission and Time-Varying Partial-Band Interference

Michael B. Pursley and Jason S. Skinner
Clemson University
Clemson, SC

ABSTRACT

A protocol is described and evaluated for adapting the rate of a turbo code for frequency-hop packet transmissions over time-varying partial-band interference channels. The rate of the turbo code is adapted from packet to packet to optimize the throughput. In particular, the protocol is designed to use a high-rate code when there is little interference and a low-rate code when the interference occupies a significant fraction of the band, even though neither the transmitter nor the receiver know what fraction of the band contains interference. No external side information is provided to the receiver, and our scheme requires no additional redundancy (e.g., pilot symbols) in the data packet for the generation of side information. The information needed to adapt the code rate is derived from our adaptive decoding system, and the only feedback required from the receiver to the transmitter is provided by a few bits in each acknowledgment packet. Results on the performance of the protocol are given for turbo product codes.

I. INTRODUCTION

We consider frequency-hop packet transmission in which there are several symbols per hop and several hops per packet. Each packet is divided into multiple segments, and the segments are transmitted in different intervals of time known as dwell intervals. All symbols in a dwell interval are transmitted in the same frequency slot, but different dwell intervals may use different frequency slots, depending on the properties of the hopping pattern. A terminal that is sending a packet employs its frequency hopping pattern to determine which frequency slot is used for each dwell interval. The use of multiple frequency slots to transmit a packet provides frequency diversity that mitigates partial-band interference and other frequency-dependent disturbances. SINCGARS [4] is an example of a frequency-hop radio system with the aforementioned features.

It has been demonstrated recently that turbo codes provide efficient error control for frequency-hop communications over channels with partial-band interference. Both parallel-concatenated turbo convolutional codes (e.g., [5] and [6]) and turbo product codes (e.g., [8] and [11]) have been shown to be superior to Reed-Solomon codes and binary convolutional codes for use in frequency-hop systems. The turbo product codes considered in this paper are particularly attractive because of their low complexity and the availability of commercial chips to perform the encoding and decoding. In [8] and [9], we show that if a suitable decoding strategy is employed, the turbo product codes provide performance that is comparable to the performance of higher-complexity turbo convolutional codes.

For the results in this paper, we employ a decoding strategy described in [9] to adaptively scale the soft decisions at the input to the decoder. The information needed to adapt the scale factor for a given dwell interval is derived from the demodulation of the received code symbols in the dwell interval. No external side information is provided, and our scheme does not require pilot symbols or any other special symbols in the data packet. Neither power measurements nor channel estimates are needed. The adaptation of the code rate depends only on the scale factors for the most recent packet reception, and the only feedback required from the receiver to the transmitter is supplied by a few bits in each acknowledgment packet.

Binary orthogonal signals are employed with soft-decision noncoherent demodulation. Our channel model is that same as the model employed in several previous investigations, including [3], [6], [8], and [11]. The primary disturbance is partial-band interference, which is modeled as band-limited white Gaussian noise that is present in a fraction ρ of the frequency slots. The one-sided power spectral density for the band-limited noise is $\rho^{-1}N_I$ in the frequency slots that have interference, and it is zero in the remaining fraction $1-\rho$ of the slots. The total power in the interference is proportional to N_I but it is independent of ρ. The partial-band noise model is convenient for use in analysis and simulation, and it represents a good approximation for many frequency-hop systems with partial-band interference [10]. The receiver's thermal noise is modeled as full-band white Gaussian noise with one-sided power spectral density N_0.

Since the number of code symbols per packet is fixed but the number of information bits per packet depends on the code that is used, our results are in terms of E_s, the energy per symbol, rather than E_b, the energy per information bit. If the transmitter power is the same for each transmission, the energy per symbol is the same, but the energy per bit changes from one transmission to the next as the code rate changes. For all of the performance results in this paper, the ratio of the energy per code symbol to

This research was supported by the U.S. Army Research Office under grant DAAD19-99-1-0289 and by the DoD MURI program under Office of Naval Research grant N00014-00-1-0565. Jason Skinner also received support from an MIT Lincoln Laboratory Fellowship.

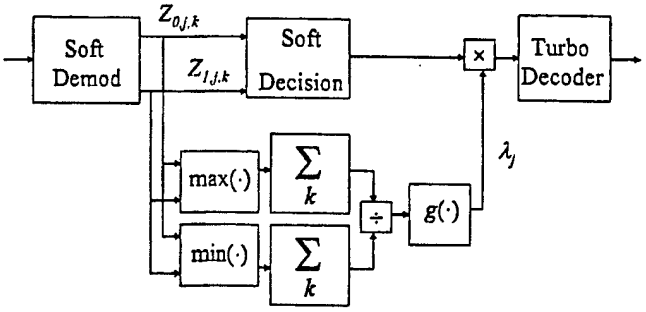

Fig. 1. Adaptive scaling

the one-sided thermal noise density is $E_s/N_0 = 19$ dB, which gives a bit-energy to noise-density ratio of approximately 20 dB for the highest-rate code. The value $E_b/N_0 = 20$ dB is used for the numerical results in [6], [8], [9] and [11].

For our performance evaluations, the value of ρ, the fraction of the band that contains interference, is constant for the duration of a packet, but it may change from one packet transmission to the next. A finite-state Markov model is employed for the time-varying fractional bandwidth. We provide comparisons between the performance of adaptive-rate turbo product coding and fixed-rate turbo product coding for the same decoding strategy.

II. The Decoding Method

The decoding system is illustrated in Fig. 1. The key feature is adaptive scaling of the demodulator's soft decisions from dwell interval to dwell interval. Our method for adaptive scaling can be used with any soft-decision decoder. The demodulator consists of a pair of noncoherent detectors (e.g., envelope detectors), one matched to each of the two binary orthogonal signals. The two binary signals and their corresponding detectors are indexed by the integer i (i=0,1). The statistic $Z_{i,j,k}$, which is nonnegative, is the output of the ith detector when the input is the kth symbol of the jth dwell interval. The soft decision for the received symbol in the kth symbol position of the jth dwell interval is based on the ratio of $Z_{1,j,k}$ to $Z_{0,j,k}$. The soft decisions can be applied directly to the decoder, but we have found that the decoder performance is improved greatly if the soft decisions are scaled according to the reliabilities of their corresponding dwell intervals. Several alternatives for scaling the soft decisions are described in [9].

For the decoding method employed in this paper, a quality measure W_j is derived from the demodulator outputs for the jth dwell interval, and the corresponding scale factor λ_j is determined from the value of W_j. As a consequence, the scale factor is adjusted within the range $0 \le \lambda_j \le 1$ to reflect the estimated quality of the symbols in the jth dwell interval. One extreme, $\lambda_j = 0$, corresponds to the erasure of all symbols in the jth dwell interval; the other extreme, $\lambda_j = 1$, corresponds to passing the soft outputs for the jth dwell interval from the demodulator to the decoder without scaling.

The quality measure is defined by

$$W_j = \frac{\sum_k \max\{Z_{0,j,k}, Z_{1,j,k}\}}{\sum_k \min\{Z_{0,j,k}, Z_{1,j,k}\}}, \tag{1}$$

where the sums are over all symbol positions within the jth dwell interval. Notice that $W_j \ge 1$. If W_j is small (i.e., close to one), the reliability is low for the soft decisions in the jth dwell interval. A large value for W_j indicates the soft decisions in the jth dwell interval are highly reliable. All soft decisions for symbols in the jth dwell interval are multiplied by $\lambda_j = g(W_j)$ for some nondecreasing function g. Thus, the soft decisions for a received packet are scaled adaptively as the packet is being received and demodulated.

Several choices for the function g were evaluated, and a linear ramp proved to be one of the best in terms of performance and robustness to channel variations. The linear ramp is defined by

$$g(w) = \begin{cases} 0, & w < w_0, \\ (w - w_0)/(w_1 - w_0), & w_0 \le w \le w_1, \\ 1, & w > w_1. \end{cases} \tag{2}$$

Thus, the graph of $g(w)$ is a linear ramp between w_0 and w_1. The parameters w_0 and w_1 are referred to as the *scaling parameters* for the adaptive decoder. Each code in the adaptive coding system may use different scaling parameters.

III. The Adaptative-Transmission Protocol

In our adaptive-transmission system, a number of codes of different rates are available for use in sending packets from one terminal, the *source*, to another terminal, the *destination*. The goal of the adaptive-transmission protocol is specified in terms of the throughput for the communication link from the source to the destination. The *throughput* is the ratio of the total number of information bits in packets that are decoded correctly at the destination to the total number of packet transmissions that are made by the source. For an information bit to be counted as a contribution to the numerator of the throughput expression, all information bits in the entire packet must be decoded correctly at the destination. However, each attempt to send a packet from the source to the destination is included in the denominator of the expression for the throughput, whether the packet is decoded correctly or not.

The adaptive-transmission protocol attempts to maximize the throughput for transmissions from the source to the destination, but the maximum achievable throughput depends on the channel conditions. For each packet transmission, the source desires to use the code of highest rate among the codes that provide the required protection against the partial-band interference that is present in the channel, but the characteristics of the partial-band interference are not known to the source. If the code rate is higher than required by the level of partial-band interference, many packets fail to decode correctly. If the code rate is lower than required by the level of partial-band interference, nearly all packets are decoded correctly, but they contain too few information bits. In either situation, the resulting throughput is low.

The adaptive-transmission protocol adjusts the code rate for the next transmission according to the decoding results for the packet that was received most recently. If the most recent packet was not decoded correctly, the destination notifies the source to switch to a lower-rate code, if possible (i.e., if the lowest-rate code was not used for the most recent packet). A high-rate CRC code is applied to each packet (such codes are common in packet transmission systems), and the decoding of the CRC code is used to verify the correctness of the received packets. If a packet is received correctly, the decoding system produces a statistic β that is used to select the code rate for the next transmission. For the determination of β, the destination counts the number of dwell intervals for which $\lambda_j \neq 1$, and it divides this by the total number dwell intervals per packet. That is, if I_j is defined by $I_j = 1$ for $\lambda_j \neq 1$ and $I_j = 0$ for $\lambda_j = 1$, then

$$\beta = \frac{1}{N} \sum_{j=1}^{N} I_j, \tag{3}$$

where N is the number of dwell intervals per packet. Notice that $I_j = 1$ implies that the soft decisions in the jth dwell interval have low reliability, so β is the fraction of the dwell intervals that have low reliability.

For the performance results on adaptive transmission given in Section V, there are at most three codes. For adaptive transmission with three codes, two adaptation parameters, β_1 and β_2, are used in the selection of the code rate for the next transmission. If $\beta < \beta_1$, the destination requests the source to use the high-rate code for the next transmission. If $\beta > \beta_2$, the destination requests the source to use the low-rate code. Otherwise, the destination requests the source to use the intermediate-rate code. If there are only two codes, there is a single adaptation parameter, which is denoted by β_0. If $\beta \leq \beta_0$, the destination requests the source to use the high-rate code for the next transmission; otherwise, it requests that the low-rate code be used. The selections of the values for β_0, β_1, and β_2 are based simulations of the turbo product codes over a range of values for E_s/N_I.

IV. Throughput for Individual Codes

The collection of codes that is used by the adaptive-rate coding system is referred to as the *code set*. In this section, four turbo product codes are evaluated for possible inclusion in the code set. For each of the four codes, we determine the throughput as a function of ρ for two values of E_s/N_I. The block length is 4096 for each code. The rates of the four codes are 0.793, 0.495, 0.325, and 0.279, corresponding to code words with 3249, 2028, 1331, and 1144 information bits, respectively. For our numerical results, there is one code word per packet, the number of dwell intervals per packet is $N = 128$, and there are 32 binary code symbols in each dwell interval.

The turbo product code of rate 0.793 is a two-dimensional code whose constituent codes are (64,57) extended Hamming codes. The code of rate 0.495 is a three-dimensional code derived from two (32,26) extended Hamming codes and a (4,3) parity-check code. The code of rate 0.325 is a three-dimensional code whose constituent codes are (16,11) extended Hamming codes,

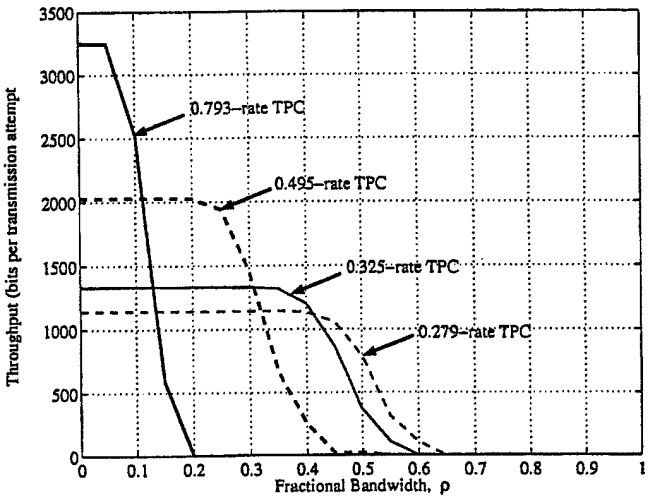

Fig. 2. Throughput for E_s/N_I = -6.0 dB

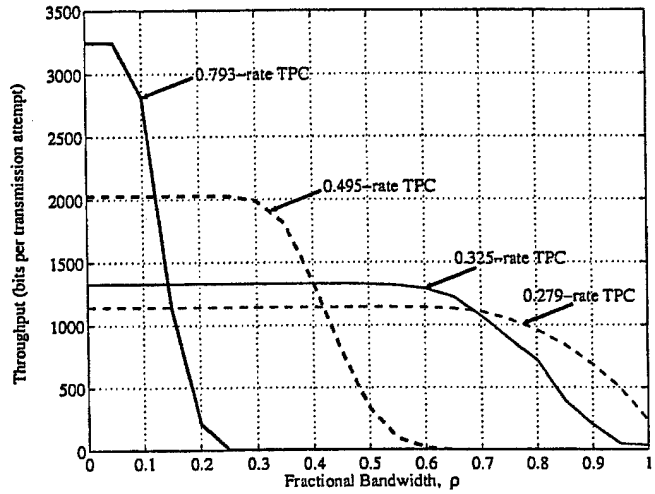

Fig. 3. Throughput for E_s/N_I = 3.0 dB

and the constituent codes for the code of rate 0.279 are the (32,26), (16,11), and (8,4) extended Hamming codes.

The results shown in Figures 2 and 3 are for $E_s/N_I = -6.0$ dB and $E_s/N_I = 3.0$ dB, respectively. Note that a small value of E_s/N_I corresponds to strong partial-band interference. For the results illustrated in these two figures, no attempt was made to optimize the scaling parameters. The scaling parameters for all four codes are $w_0 = 2$ and $w_1 = 5$. For each graph, we see that the highest-rate code gives the greatest throughput if ρ is small, but the lowest-rate code gives the greatest throughput if ρ is large. The range of ρ over which the lowest-rate code is optimum and the amount of additional throughput it provides (compared to the code of rate 0.325) are so small that there is not much to be gained by including it in the code set. However, among the other three codes, the results in Figures 2 and 3 show that each has a very large performance advantage over the other two for one interval of values of ρ.

We also investigated the optimum pair of scaling parameters for each code. We found that the optimum scaling parameters

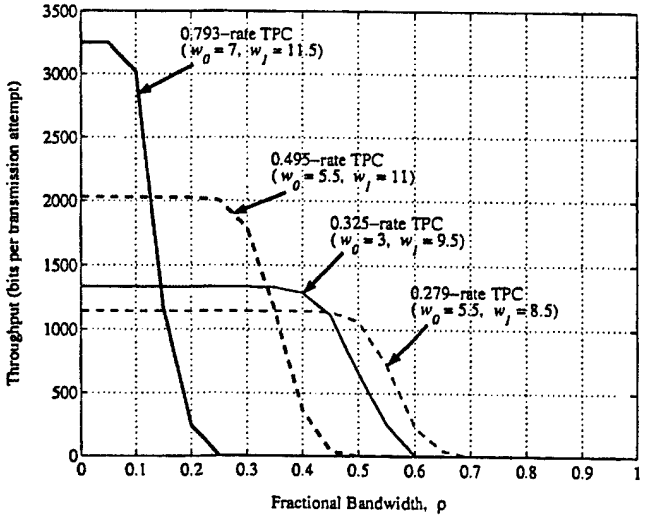

Fig. 4. Throughput for E_s/N_I = -6.0 dB

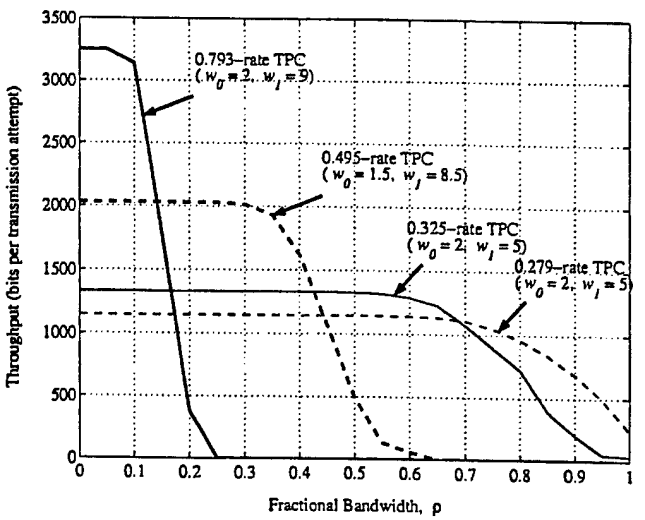

Fig. 5. Throughput for E_s/N_I = 3.0 dB

depend on the value of E_s/N_I. For $E_s/N_I = -6.0$ dB, we see from Figure 4 that the increase in throughput is not significant for most values of ρ; however, the increase is large for a few intervals (e.g., the interval around $\rho = 0.1$ for the high-rate code). Notice that the scaling parameters listed in Figure 4 are larger than the values $w_0 = 2$ and $w_1 = 5$ used for Figures 2 and 3. Larger scaling parameters give a smaller set of scale factors λ_j for the same set of quality measures W_j. Thus, for example, an adaptive decoder with a large value of w_0 erases more dwell intervals than an adaptive decoder with a small value of w_0.

From Figure 5, we see that the differences between the optimum scaling parameters and the values $w_0 = 2$ and $w_1 = 5$ are smaller for $E_s/N_I = 3.0$ dB than for $E_s/N_I = -6.0$ dB. In addition, the optimum parameter values for $E_s/N_I = 3.0$ dB are smaller than the optimum values for $E_s/N_I = -6.0$ dB. One consequence is that the optimum parameters for $E_s/N_I = 3.0$ dB (relatively weak interference) result in fewer erasures than produced by the optimum parameters for $E_s/N_I = -6.0$ dB (relatively strong interference), which is as expected. The optimum value for w_0 for the high-rate code is $w_0 = 2$, the same as the value used for Figures 2 and 3. However, the optimum values of w_1 for the high-rate code are larger than $w_1 = 5$, and we see from Figures 4 and 5 that these larger values give improved throughput in the interval around $\rho = 0.1$.

V. Performance Results for Adaptive Transmission

As discussed in the previous section, the code set could have as many as four turbo product codes of block length 4096, but the lowest-rate code would rarely be selected by a protocol that attempts to maximize the throughput. Therefore, the largest code set employed for the results in this section has three codes whose rates are 0.793, 0.495, and 0.325. For the results in Figures 7, 10, 11, and 12, the scaling parameters are $w_0 = 2$ and $w_1 = 5$, and the adaptation parameters are $\beta_0 = 0.11$, $\beta_1 = 0.11$, and $\beta_2 = 0.3$.

In order to generate time-varying interference in our simulations, we use finite-state Markov models in which each state corresponds to a different value of ρ. In each Markov model, state 0 has no interference, which is obtained by letting the value of ρ for state 0 be $\rho_0 = 0$. Each of the other states corresponds to a positive value of ρ. The state is constant during the transmission of a packet, but the state may change from one transmission to the next.

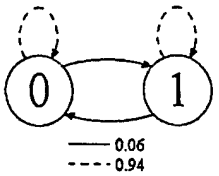

Fig. 6. Two-state Markov chain (ρ_0 = 0, ρ_1 = 0.25)

The first set of performance results is for the two-state Markov model illustrated in Figure 6. When the channel is in state 1, there is partial-band interference in a fraction $\rho_1 = 0.25$ of the frequency band. The state transition probabilities are 0.06 and 0.94, as shown in Figure 6. The performance results for adaptive-rate coding for the two-state Markov model are shown in Figure 7. The throughput is shown as a function of E_s/N_I for two code sets. One code set includes all three codes and the other has only the codes of rates 0.793 and 0.325. The inclusion of the code of rate 0.495 in the first set permits the adaptive-rate coding system to use this code when the channel is in state 1, whereas the adaptive-rate coding system that has only two codes is typically using the code of rate 0.325 when the channel is in state 1. This accounts for the improved throughput for the system with three codes when E_s/N_I is less than approximately 10 dB. An examination of Figures 2–5 shows that for $\rho = 0.25$, the code of rate 0.495 is superior to the code of rate 0.325, and the code of rate 0.793 is inferior to both of these codes.

The second and third Markov models have four states, as illustrated in Figures 8 and 9. When each of these is in state i, $0 \le i \le 3$, there is partial-band interference in a fraction ρ_i of the band. The state transition probabilities for the four-state

Markov model shown in Figure 8 are 0.03, 0.94, and 0.97, and the state transition probabilities for the Markov model shown in Figure 9 are 0.02 and 0.94. Performance results for adaptive-rate coding for each of the two four-state Markov models are illustrated in Figure 10 for $\rho_0 = 0$, $\rho_1 = 0.125$, $\rho_2 = 0.25$, and $\rho_3 = 0.5$, and in Figure 11 for $\rho_0 = 0$, $\rho_1 = 0.1$, $\rho_2 = 0.2$, and $\rho_3 = 0.4$. In each figure, the throughput is shown as a function of E_s/N_I for a code set that consists of the turbo product codes of rates 0.793, 0.495, and 0.325.

In Figures 10 and 11, there is very little difference in performance between the two Markov models over the entire range of values of E_s/N_I. In Figure 10, as the value of E_s/N_I decreases to -20 dB, the throughput decreases to approximately 1800 bits per packet for both Markov models. In Figure 11, as the value of E_s/N_I decreases to -20 dB, the throughput decreases to approximately 2100 bits per packet for each model. The smaller values for ρ_1, ρ_2, and ρ_3 used for Figure 11 permit more frequent use of higher-rate codes, which accounts for the higher throughput for strong partial-band interference (i.e., small values of E_s/N_I) in Figure 11 compared to Figure 10.

In Figure 12, we compare the throughput for our adaptive-rate coding technique with the throughput for fixed-rate coding. The results shown for fixed-rate coding are for the codes of rates 0.793 and 0.495. For each value of E_s/N_I, the throughput achieved by either of the two lowest-rate codes is less than that for either of the two highest-rate codes, so the throughput curves are not shown for the codes of rates 0.325 and 0.279. The adaptive-rate coding system achieves much higher throughput for the entire range of value of E_s/N_I shown in Figure 12 than can be obtained from fixed-rate coding using the code of rate 0.495. For $E_s/N_I < 7$ dB, the adaptive-rate coding system also achieves much larger throughput than is achievable with fixed-rate coding using the code of rate 0.793. For $E_s/N_I > 15$ dB, the adaptive-rate system achieves the same throughput as the code of rate 0.793; however, for E_s/N_I between 7 dB and 15 dB, the code of rate 0.793 has a higher throughput than the adaptive-rate coding system. This suggests that different adaptation parameters should be used if it is desired to maximize the throughput for E_s/N_I in the range from 7 to 15 dB.

We found that the adaptive coding system can achieve higher throughput for E_s/N_I in the range from 7 to 15 dB if the adaptation parameters are increased. We also adjusted the scaling parameters to increase the throughput for each code. Of course, the improvement in the scaling parameters increases the throughput for the adaptive coding system and for the individual fixed-rate codes. For the results in Figure 13, the pairs (w_0,w_1) of scaling parameters are (2.0,9.0), (1.5,8.5), and (2.0,9.5), for the codes of rates 0.793, 0.495, and 0.325, respectively. The adaptation parameters are $\beta_1 = 0.5$ and $\beta_2 = 0.65$.

Comparison with the fixed-rate results shows that the throughput is now almost uniformly higher for adaptive-rate coding than for either fixed-rate code. The one exception is the interval from approximately 10 to 11 dB, where the throughput is slightly larger for the high-rate code. For E_s/N_I greater than 11 dB, the throughput of the adaptive coding system is nearly equal

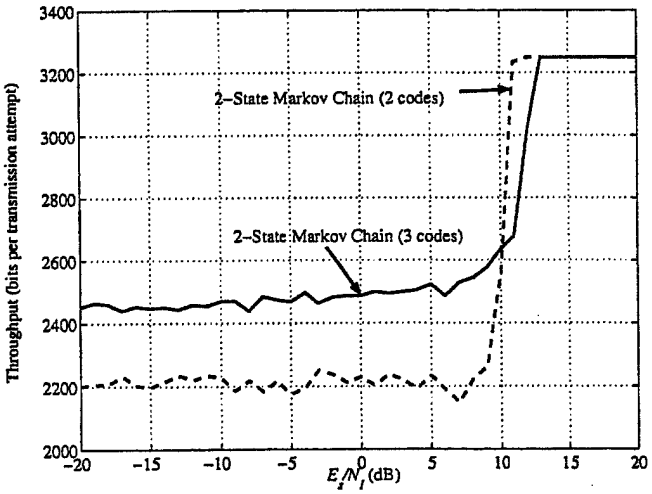

Fig. 7. Throughput for $\rho_0 = 0$ and $\rho_1 = 0.25$

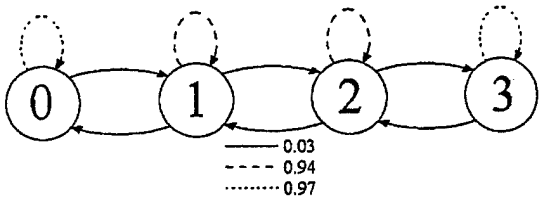

Fig. 8. Four-state Markov chain 1

to 3249 bits per transmission attempt, which is the maximum possible throughput for any coding system that has a maximum rate of 0.793. (Note that 3249 is the number of information bits per packet for a code of rate 0.793 and block length 4096.) This maximum is attained by the adaptive-rate coding system for E_s/N_I greater than 12 dB, and the adaptive system also achieves a 15% larger throughput than each of the fixed-rate codes for all values of E_s/N_I less than 7 dB.

VI. Conclusions

The protocol for adaptive-rate coding that is described and evaluated in this paper is suitable for a wide range of codes and soft-decision decoders. In particular, the protocol can be used with binary convolutional coding or any form of turbo coding. Although our numerical results are for turbo product codes, neither the code structure nor the decoding algorithm play a role in the adaptation of the code rate. Our results demonstrate

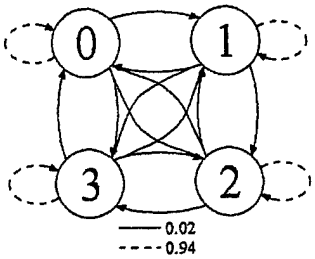

Fig. 9. Four-state Markov chain 2

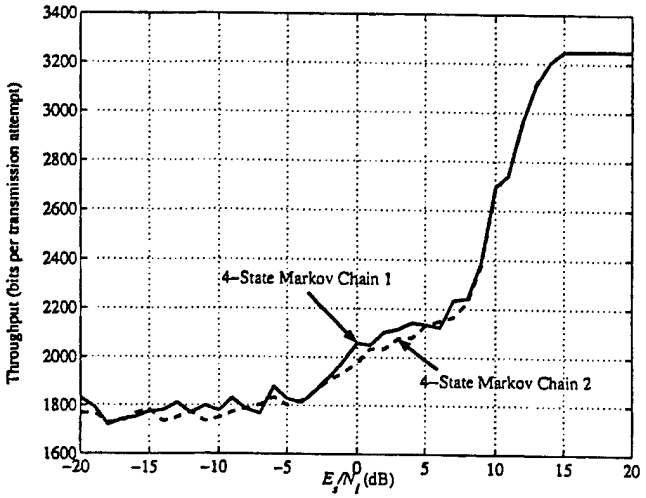

Fig. 10. Throughput for $\rho_0 = 0$, $\rho_1 = 0.125$, $\rho_2 = 0.25$, $\rho_3 = 0.5$

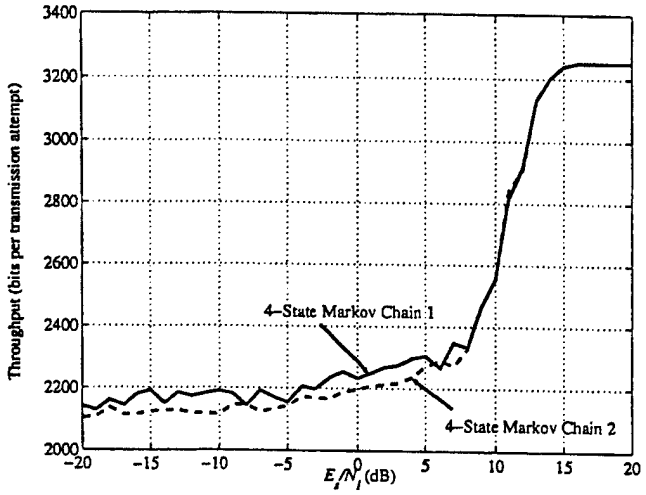

Fig. 11. Throughput for $\rho_0 = 0$, $\rho_1 = 0.1$, $\rho_2 = 0.2$, $\rho_3 = 0.4$

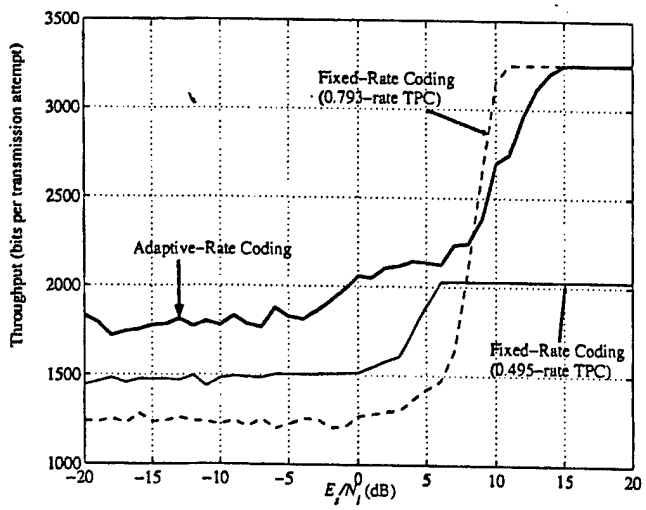

Fig. 12. Four-state Markov chain 1 ($\rho_0 = 0$, $\rho_1 = 0.125$, $\rho_2 = 0.25$, $\rho_3 = 0.5$)

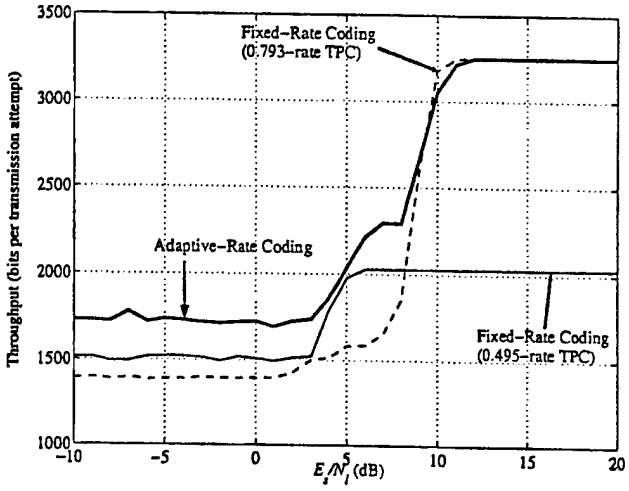

Fig. 13. Four-state Markov chain 1 ($\rho_0 = 0$, $\rho_1 = 0.125$, $\rho_2 = 0.25$, $\rho_3 = 0.5$)

the feasibility of the adaptive-rate coding technique and the performance advantages of adaptive-rate coding over fixed-rate coding for channels with time-varying interference. In particular, the adaptive-rate coding system obtains the maximum possible throughput when channel conditions are good and it provides better throughput than fixed-rate coding when channel conditions are poor.

REFERENCES

[1] Advanced Hardware Architectures, Inc., Product Specification for AHA4501 Astro 36 Mbits/sec Turbo Product Code Encoder/Decoder. Pullman, WA. Available: http://www.aha.com

[2] Efficient Channel Coding, Inc., Product Summary: AHA4501 Astro Turbo Product Code Evaluation Module. Brooklyn Heights, OH. Available: http://www.eccincorp.com

[3] C. D. Frank and M. B. Pursley, "Concatenated coding for frequency-hop spread-spectrum with partial-band interference," *IEEE Transactions on Communications*, vol. 44, pp. 377-387, March 1996.

[4] B. J. Hamilton, "SINCGARS system improvement package (SIP) specific radio improvements," *Proceedings of the 1986 Tactical Communications Conference*, pp. 397-406, April 1996.

[5] J. H. Kang and W. E. Stark, "Turbo codes for coherent FH-SS with partial band interference," *Proceedings of the 1997 Military Communications Conference*, vol. 1, pp. 5-9, November 1997.

[6] J. H. Kang and W. E. Stark, "Turbo codes for noncoherent FH-SS with partial band interference," *IEEE Transactions on Communications*, vol. 46, pp. 1451-1458, November 1998.

[7] M. B. Pursley, "Reed-Solomon codes in frequency-hop communications," Chapter 8 in *Reed-Solomon Codes and Their Applications*, S. B. Wicker and V. K. Bhargava (eds.), pp. 150-174, IEEE Press, New York, 1994.

[8] M. B. Pursley and J. S. Skinner, "Turbo product coding in frequency-hop wireless communications with partial-band interference," *Proceedings of the 2002 IEEE Military Communications Conference* (Anaheim, CA), pp. U405.5.1-6, October 2002.

[9] M. B. Pursley and J. S. Skinner, "Decoding strategies for turbo product codes in frequency-hop wireless communications," *Proceedings of the 2003 IEEE International Conference on Communications* (Anchorage, AK), vol. 4, pp. 2963-2968, May 2003.

[10] A. J. Viterbi and I. M. Jacobs, "Advances in coding and modulation for noncoherent channels affected by fading, partial band, and multiple-access interference," in *Advances in Communication Systems: Theory and Applications*, vol. 4, A. J. Viterbi (ed.), pp. 279-308, Academic Press, New York, 1975.

[11] Q. Zhang and T. Le-Ngoc, "Turbo product codes for FH-SS with partial-band interference," *IEEE Transactions on Wireless Communications*, vol. 1, no. 3, pp. 513-520, July 2002.